Hindawi

Research Article

Abnormal Health Monitoring and Assessment of a Three-Phase Induction Motor Using a Supervised CNN-RNN-Based Machine Learning Algorithm

Abhinav Saxena [1] **Rajat Kumar** [2] **Arun Kumar Rawat** [1] **Mohd Majid** [3] **Jay Singh** [4] **S. Devakirubakaran** [5] **and Gyanendra Kumar Singh** [6]

[1]*Department of Electrical Engineering, JSS Academy of Technical Education, Noida, Uttar Pradesh, India*

[2]*Department of Electrical Engineering, Dayalbagh Educational Institute, Dayalbagh, Uttar Pradesh, Agra, India*

[3]*Department of Mechanical Engineering, Sant Longowal Institute of Engineering and Technology, Longowal, Sangrur, Punjab, India*

[4]*Department of Electrical and Electronics Engineering, GL Bajaj Institute of Technology and Management, Noida, Uttar Pradesh, India*

[5]*Dapartment of Electrical and Electronics Engineering, QIS College of Engineering and Technology, Ongole, Andhra Pradesh, India*

[6]*School of Mechanical, Chemical and Materials Engineering, Adama Science and Technology University, Adama, Ethiopia*

Correspondence should be addressed to Gyanendra Kumar Singh; gksinghgu@yahoo.com

This paper shows the health monitoring and assessment of a three-phase induction motor in abnormal conditions using a machine learning algorithm. The convolutional neural network (CNN) and recurrent neural network (RNN) algorithms are the prominent methods used in machine learning algorithms, and the combined method is known as the CRNN method. The abnormal conditions of a three phase-induction motor are represented by three-phase faults, line-to-ground faults, etc. The pattern of fault current is traced, and key features are extracted by the CRNN algorithm. The performance parameters like THD (%), accuracy, and reliability of abnormal conditions are measured with the CRNN algorithm. The assessment of abnormal conditions is being realized at the terminals of a three-phase induction motor. A fuzzy logic controller (FLC) is also used to assess such abnormalities. It is observed that performance parameters are found to be better with the CRNN method in comparison to CNN, RNN, ANN, and other methods. Such a realization makes the system more compatible with abnormality recognition.

1. Introduction

Induction motors are one of the most versatile and frequently used variable-speed drives for industrial and domestic applications. Normally, the three-phase supply-based induction motor is used to drive heavy loads. The major challenge with the induction motor is maintaining the normal supply. The changing loads, fault conditions, and overspeeding affect the supply and create abnormalities that can be assessed using the machine learning algorithm. The monitoring aspect of machine failure diagnostics is important, and for recognizing a failure in mechanical systems, classifying the error, and recognizing group faults, numerous sensors are installed to gather information from thermal imaging or vibration. Afterward, these data are analyzed to see whether a defect has occurred or not, and if so, what kind of fault it is.

Traditionally, to identify a machine's malfunction, a sensor is required for signal acquisition, feature selection, and fault categorization, as well as extraction. Sensing data

acquisition entails gathering sensor data while the device in use is active. Conventional extracted features include original sensor data from time data in both the temporal and frequency domains. A new framework for deep learning is proposed to achieve very accurate machine fault detection and to understand how to facilitate and expedite deep neural network training networks. In comparison to current techniques, the suggested technique is more accurate and quicker to train. The initial sensor data are utilized using wavelet transformation to turn the data into pictures, followed by assembling the time-frequency distributions. Then, a trained network is applied to extract more fundamental features, including the time-frequency label [1–5]. The higher tiers of the algorithm are then fine-tuned using photographs and neural network design. The document causes a bug in the system, in which experiments and a diagnosis pathway are used to confirm the pipeline's efficiency and applicability in general on three fundamental mechanical data sets containing gearboxes, induction motors, and bearings with three-time series samples of different sizes [6–11].

The proposed method can be used to diagnose faults in rotary machine systems' exterior bearings and uses deep learning and information fusion. The suggested method takes as its direct input raw signals from various phases of the motor current, from which features are then retrieved. Afterward, CNN classifies each feature set separately for the network of neurons. An innovative decision-level information fusion strategy is presented to combine data from all of the used convolutional neural networks in order to improve classification accuracy. CNN provides higher accuracy in its image recognition pattern and a better approach to automatically detecting important features without any human supervision. On the contrary, RNN produces the sequential output, which depends on time-sequence events. Decision-level data processing has difficulty because of straightforward pattern categorization problems that can be efficiently solved by well-known supervised learning algorithms. The suggested fault diagnosis product's efficacy is validated by tests that used genuine bearing fault signals [12–14]. This work describes a technique for identifying bearing defects and tracking bearing deterioration in electric motors. The method collects fault features that reflect various faults based on signal kurtosis and cross-correlation, and the characteristics are then integrated to create a health index using hierarchical clustering and a semisupervised k-nearest neighbour distance measure. Experiments with a computer cooling fan motor bearing and a simulator for machinery faults were used to validate the method. The technique can locate defects under masking noise and diagnose faults in their early stages. Additionally, it offers a health index that monitors fault degeneration while excluding intermittent defects. Furthermore, inaccurate reference data are not necessary [15–18]. In theory, sophisticated artificial intelligence-based systems provide early fault identification, but their complexity conflicts with instant messaging are fundamental characteristics.

This manuscript utilizes the motor current signature, which is already present in standard drives, and proposes a

combination of simulations and upsampling to practice the neural network effectively without any need for numerous broken prototypes, which is the main obstacle to industrial viability [19–22]. Deep conviction systems for biomedical applications using intuitive procedures with a cross-point approach are analyzed. The mechanism of the Internet of things (IoT) integrated with radio frequency identification (RFID) technology for healthcare systems gives fruitful information. Biomedical signals for healthcare using Hadoop infrastructure with artificial intelligence and fuzzy logic interpretation show the health analysis [23–25]. An induction motor driven by an inverter and its diagnosis using a machine learning algorithm are well analyzed. With the help of growing curvilinear component analysis, the stator of an induction motor helps to track the fault at the grid terminal. A diagnosis of the IGBT converter and current sensor fault for the inverter-driven induction motor using the online Simulink method is well explained in [26–28].

2. Mathematical Modeling of Three-phase Induction Motor

The mathematical modeling of a three-phase induction motor is designed in the d-q reference frame coordinates. The conversion of three-phase coordinates to $(d–q)$ coordinates is assessed using the Clarke and Park transformation. In the Clarke transformation, three-phase (a, b, and c) coordinates are converted into stationary reference coordinates ($\alpha–\beta$). A further Park transformation is used to convert the stationary reference coordinates ($\alpha–\beta$) into synchronous reference frame coordinates ($d–q$). The mathematical modeling of a three-phase induction motor is represented as

$$V_{sd} = R_s i_{sd} + \frac{d}{dt}\phi_{sd} - \omega_s \phi_{sq}$$

$$V_{sq} = R_s i_{sq} + \frac{d}{dt}\phi_{sq} + \omega_s \phi_{sq}$$

$$V_{rd} = R_r i_{rd} + \frac{d}{dt}\phi_{rd} - \omega_r \phi_{rq}$$

$$V_{rq} = R_r i_{rq} + \frac{d}{dt}\phi_{rq} + \omega_r \phi_{rd} \, , \qquad (1)$$

$$\phi_{sd} = L_s i_{sd} + L_m i_{rd}$$

$$\phi_{sq} = L_s i_{sq} + L_m i_{rq}$$

$$\phi_{rd} = L_s i_{rd} + L_m i_{sd}$$

$$\phi_{rq} = L_s i_{rq} + L_m i_{sq}$$

where V_{sd} and i_{sd} are d-axis stator voltage and stator current, respectively. V_{rd} and i_{rd} are d-axis rotor voltage and rotor current, respectively. V_{sq} and i_{sq} are q-axis stator voltage and

stator current, respectively. V_{rq} and i_{rq} are q-axis rotor voltage and rotor current, respectively.

The torque equation is given by

$$T_e - T_L = J \frac{d(\omega_r)}{dt}. \tag{2}$$

Electromagnetic torque is given by

$$T_e = p(\phi_{sd} i_{sq} - \phi_{sq} i_{sd}), \tag{3}$$

where p is the pole pair.

The general structure of a grid-connected three-phase induction motor is shown in Figure 1.

3. Design of the Convolution Neural Network (CNN)

CNN is defined as a product of the two inputs in the real-time domain. A particular kind of feedforward neural network is the convolutional neural network (CNN). It can be used for target recognition, segmentation, and image classification, among other things. The CNN model is different from other neural networks in that it has convolutional and pooling layers. The feedforward network can be illustrated as a function, as given in the following equation:

$$Y = f(X, f). \tag{4}$$

where $X = [x)_1, x_2, x_3, \ldots x_n]$ are inputs vectors. $Y = [y)_1, y_2, y_3, \ldots y_n]$ are output vectors. f is the faulty current at the different level.

The convolution layer's goal is to derive local characteristics from input data, as shown in the following equation:

$$Y_F = \text{conv}(Y, f). \tag{5}$$

$$Y_F = \text{conv}(Y, \text{convf}). \tag{6}$$

Conv is a convolution layer, Y_F is a set of extracted features, and extraction of the convolution layer from X. Y_f is the set of extracted features after the pooling layer. CNN has Softmax layers to integrate and categorize features as part of a classification model. The compressed features of the output are given as Y_{ff}, as shown in the following equation:

$$Y_F = \text{pool}(Y_F, \text{poolf}),$$
$$Y_{FF} = \text{Soft max}(FC, (Y_F, \text{poolf})). \tag{7}$$

The architecture of CNN with a pooling layer is shown in Figure 2, and data extraction from Table 1 process is shown in Figure 3.

4. Design of the Recurrent Neural Network (RNN)

RNNs are a variety of feedforward neural networks . RNN is most often used for data that has a sequence, for example in speech recognition and translation software. A popular RNN model was the LSTM LSTM-RNN, which uses memory cells to retain long-term data to address the issue of vanishing gradients. As a classification algorithm, LSTM-RNN
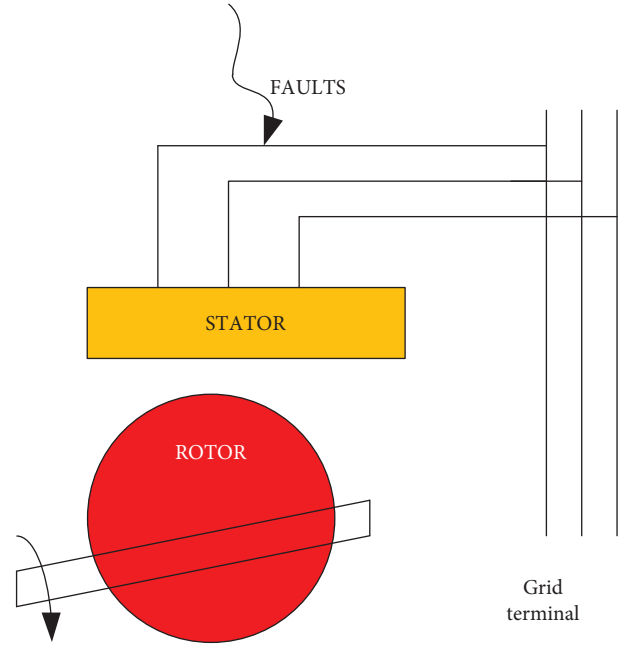

FIGURE 1: Structure of a grid-connected three-phase induction motor [6].

additionally includes Softmax layers as well as full levels [22]. The architecture of the RNN is shown in Figure 4. The normalized output of the RNN is represented mathematically, as shown in the following equation:

$$Y_{FF} = \text{Soft max}(F)C(LSTM(Y_F, \text{poolf})). \tag{8}$$

5. Design of the Convolution Recurrent Neural Network (CRNN)

CRNN is a combination of CNN and RNN. The effectiveness of CNN-based models in utilizing geographic information characteristics, such as those seen in photographs, is good. CNN, unfortunately, is unable to handle sequential data. RNN-based models, on the other hand, excel at modeling sequential data, such as texts. A novel model called CRNN is suggested, which combines CNN and RNN and is influenced by their traits. The characteristics of the inputs are extracted by the CNN, and the retrieved features are further processed by the RNN to lessen the dependence on variables under various variable situations. By eliminating the ambiguity and boundary conditions of the images, it investigates the options one at a time [22]. The general equations of CRNN are listed in the following equations:

$$i_t = \sigma(W)_{iw}x_t + U_{ih}h_{t-1} + b_i), \tag{9}$$

$$f_t = \sigma(W)_{fw}x_t + U_{fh}h_{t-1} + b_f), \tag{10}$$

$$o_t = \sigma(W)_{ow}x_t + U_{oh}h_{t-1} + b_o), \tag{11}$$

$$g_t = \tanh(W)_{gw}x_t + U_{gh}h_{t-1} + b_g), \tag{12}$$
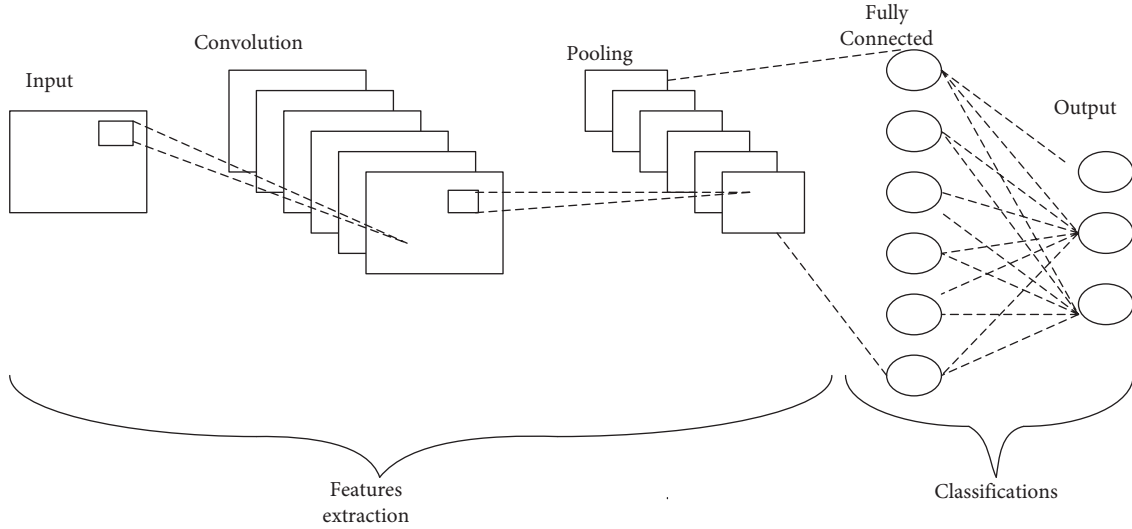
$$c_t = f_t \circ c_{t-1} + i_t \circ g_t, \tag{13}$$

FIGURE 2: Architecture of the CNN [1].

TABLE 1: Fault level at various conditions.

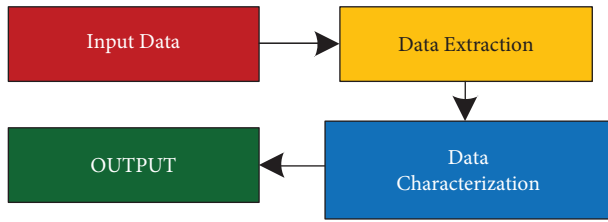| Level (f)	L1	L2	L3	L4	L5	L6	L7	L8	L9
Three-phase fault	1	0	1	0	1	1	1	0	0
Line to ground fault	0	1	1	1	0	0	1	1	0
Line to line fault	1	1	0	0	0	1	1	1	0

FIGURE 3: Data extraction of the CNN [2].

$$h_t = o_\text{t} \circ \tanh c_\text{t}, \tag{14}$$

where t is the LSTM step. xt is the input data. ht is the hidden data. ct is the cell state. it, ft, and ot are the input gate, forget gate, and output gate, respectively. Ws, Us, and bs are the weights and bias. σ, tanh, $\circ$ are sigmoid functions, hyperbolic tangents, and multiplicators, respectively. The mixed solution of CNN and RNN in mathematical form for evaluating the various fault conditions of a three-phase induction motor is shown as

$$Y_\text{FF} = \text{Soft max}\left(FC\left(\text{LSTM}\left(Y_F, \text{poolf}\right), \right.\right. \\ \left.\left. \text{conv}\left(Y, \text{convf}\right), \text{pool}\left(Y_F, \text{poolf}\right)\right). \tag{15}$$

The architecture of the problem solution of CRNN is shown in Figure 5. The forget gate is mathematically represented by $c_t{}^f = f_t o c_{t-1}$, which means that it is the dot product of the convolution of two inputs. While taking the dot product of two inputs, a few elements are removed from the output, which can be forgotten. LSTM is a long short-term memory that is an extended part of an RNN, and it occurs when gradient failure.

6. Result and Performance Analysis of the Abnormal Condition

In previous sections, the designs of CNN, RNN, and CRNN have been discussed in detail. Now, the performance parameters like THD (%), accuracy, and reliability will be estimated for the performance analysis of the single and multilabeling data. The comparison of THD (%) of fault current for single and multilabeling data is shown in Table 2. Such a graphic comparison is also depicted in Figure 6. In the same way, a comparison of the accuracy of fault current for single and multilabeling data is shown in Table 3 for the precision of 1.2% and 1.9%. Such a graphic comparison is also depicted in Figure 7.

In the same way, a comparison of the reliability of fault current for single and multilabeling data is shown in Table 4 for the precisions of 1.2% and 1.9%. Such a graphic comparison is also depicted in Figure 8.

It is observed that in Figures 6–8, the least and improved values of THD (%), accuracy, and reliability are attained with CRNN in comparison to CNN, RNN, and ANN [19]. THD is defined as total harmonic distortion, which is represented as

$$\text{THD} = \sqrt{\frac{1}{g^2} - 1}, \tag{16}$$

where g is the distortion factor, which is given in the following equation:

$$g = \frac{(X_{01})_\text{rms}}{(X)_\text{rms}}, \tag{17}$$

where X_{01} is the fundamental harmonic component, and X1 is the rms input value.

7. Conclusion

This study uses a machine learning method to monitor and evaluate a three-phase induction motor's health when it is in an aberrant state. The CRNN approach, which combines the well-
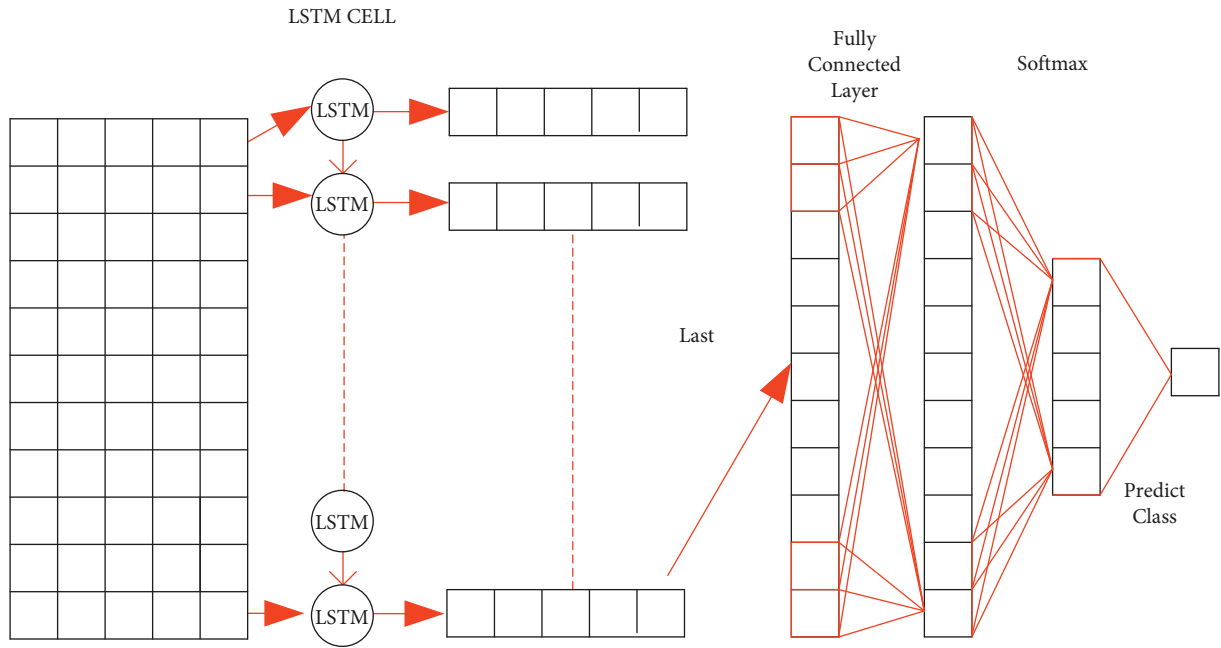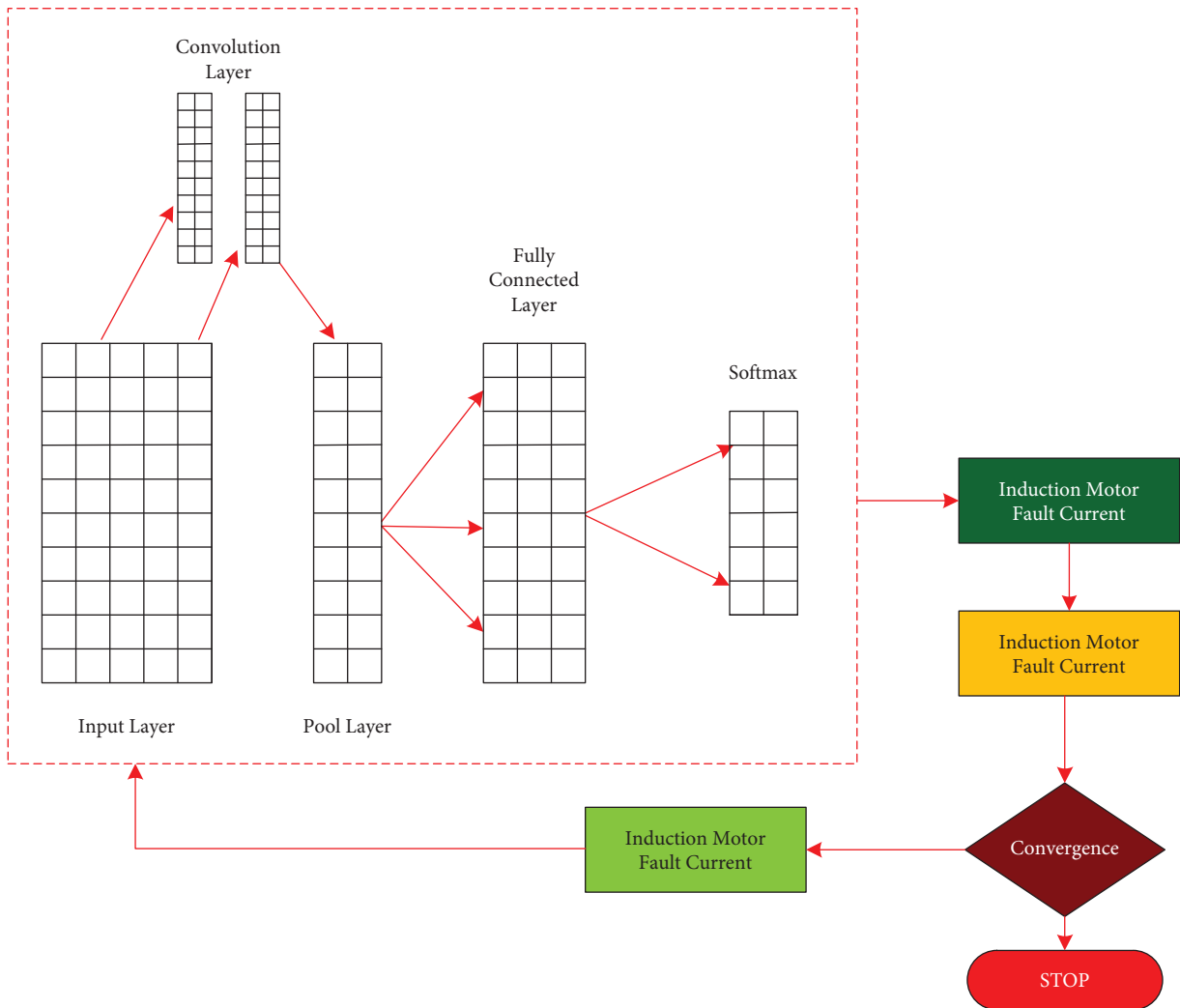
FIGURE 4: Architecture of the RNN [22].

FIGURE 5: Architecture of the CRNN.

TABLE 2: Comparison of THD (%) of fault current with various methods.

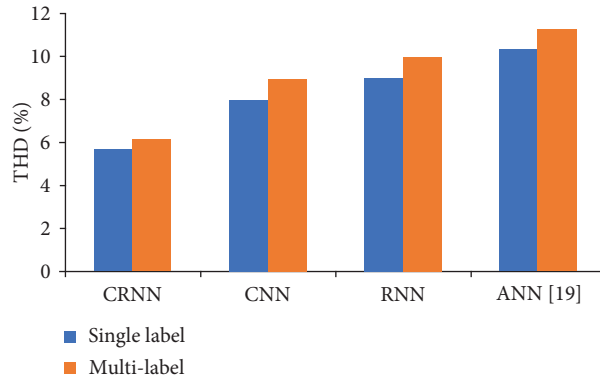| Data	CRNN	CNN	RNN	ANN [19]
Single label	5.66	7.98	8.98	10.33
Multilabel	6.12	8.97	9.98	11.22

FIGURE 6: Graphical comparison of THD (%) with various methods.

TABLE 3: Comparison of the accuracy of fault current with various methods.

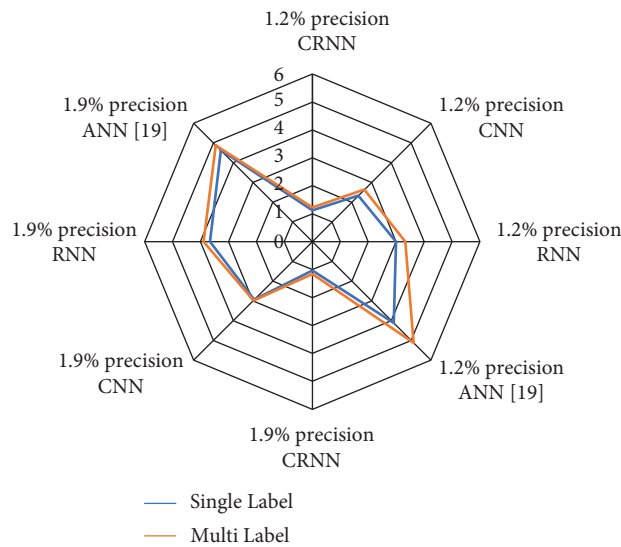| Data	1.2% precision				1.9% precision			
	CRNN	CNN	RNN	ANN [19]	CRNN	CNN	RNN	ANN [19]
Single label	1.36	2.36	2.66	3.69	1.56	2.98	3.78	4.65
Multilabel	1.45	2.89	3.21	4.23	1.61	2.91	3.06	4.02

FIGURE 7: Graphical comparison of reliability with various methods for different precision values.

TABLE 4: Comparison of reliability of fault current with various methods.

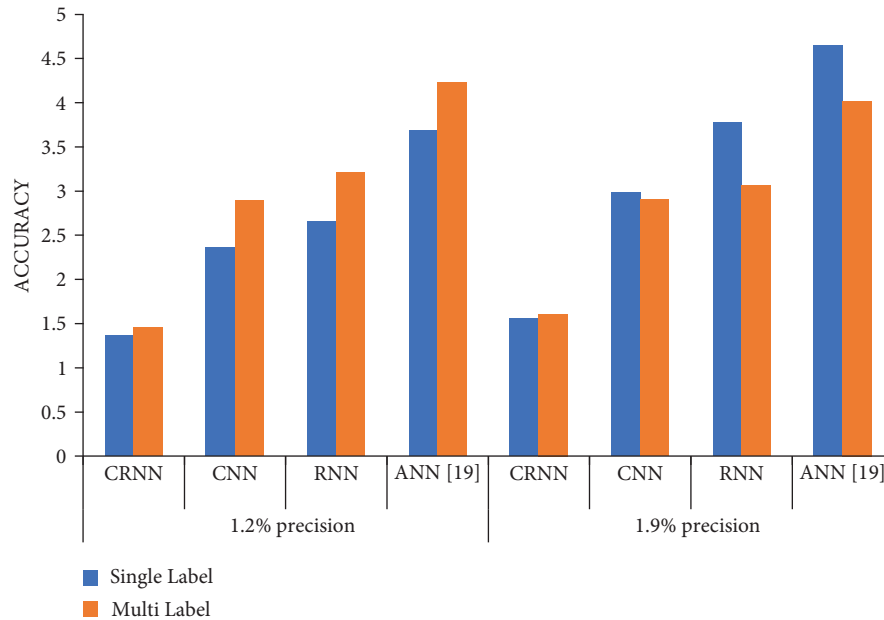| Data	1.2% precision				1.9% precision			
	CRNN	CNN	RNN	ANN [19]	CRNN	CNN	RNN	ANN [19]
Single label	1.12	2.33	2.99	4.12	1.03	2.94	3.66	4.63
Multilabel	1.23	2.64	3.33	5.12	1.16	2.98	3.89	4.88

FIGURE 8: Graphical comparison of accuracy with various methods for different precision values.

known CNN and RNN algorithms, is one of the main machine learning algorithms. Three-phase faults and line-to-ground faults, are some of the abnormal conditions of a three-phase induction motor. By using the CRNN technique, the fault current's pattern is tracked and its main features are retrieved. With the CRNN algorithm, performance metrics including THD (%), accuracy, and reliability of abnormal conditions are measured. Also, the performance metrics including THD (%), accuracy, and reliability of abnormal conditions are measured. This abnormal condition assessment is realized at the terminals of a three-phase induction motor. An artificial neural network (ANN) is also used to evaluate this irregularity. When compared to ANN, RNN, CNN, and other approaches, the CRNN method is proven to have better performance metrics. This realization improves the system's ability to detect abnormalities.

8. Future Scope

It is also a possibility that performance parameters like THD (%), accuracy, and reliability of abnormal conditions can be improved by using other advanced methods for the perfect recognition of abnormal conditions in induction motors.

Data Availability

No data were used to support the study.

Conflicts of Interest

The authors declare that they have no conflicts of interest.

References

[1] S. Shao, S. McAleer, R. Yan, and P. Baldi, "Highly-accurate machine fault diagnosis using deep transfer learning," *IEEE Transactions on Industrial Informatics*, vol. 15, no. 4, pp. 2446–2455, 2019.

[2] C. Shimmin, P. Sadowski, P. Baldi et al., "Decorrelated jet substructure tagging using adversarial neural networks," *Physical Review D*, vol. 96, no. 7, Article ID 074034, 2017.

[3] D. Fooshee, A. Mood, E. Gutman et al., "Deep learning for chemical reaction prediction," *Molecular Systems Design & Engineering*, vol. 3, no. 3, pp. 442–452, 2018.

[4] C. N. Magnan and P. Baldi, "SSpro/ACCpro 5: almost perfect prediction of protein secondary structure and relative solvent accessibility using profiles, machine learning, and structural similarity," *Bioinformatics*, vol. 30, no. 18, pp. 2592–2597, 2014.

[5] P. Baldi, "Deep learning in biomedical data science," *Annual Review of Biomedical Data Science*, vol. 1, pp. 181–205, 2018.

[6] W. Sun, S. Shao, R. Zhao, R. Yan, X. Zhang, and X. Chen, "A sparse auto-encoder based deep neural network approach for induction motor faults classification," *Measurement*, vol. 89, pp. 171–178, 2016.

[7] X. Ding and Q. He, "Energy-fluctuated multiscale feature learning with deep convnet for intelligent spindle bearing fault diagnosis," *IEEE Transactions on Instrumentation and Measurement*, vol. 66, no. 8, pp. 1926–1935, 2017.

[8] R. Zhao, D. Wang, R. Yan, K. Mao, F. Shen, and J. Wang, "Machine health monitoring using local feature-based gated recurrent unit networks," *IEEE Transactions on Industrial Electronics*, vol. 65, no. 2, pp. 1539–1548, 2018.

[9] S. J. Pan and Q. Yang, "A survey on transfer learning," *IEEE Transactions on Knowledge and Data Engineering*, vol. 22, no. 10, pp. 1345–1359, 2010.

[10] L. Wen, L. Gao, and X. Li, "A new deep transfer learning based on sparse autoencoder for fault diagnosis," *IEEE Transactions on Systems, Man, and Cybernetics: Systems*, vol. 49, no. 1, pp. 136–144, 2019.

[11] F. Shen, C. Chen, R. Yan, and R. X. Gao, "Bearing fault diagnosis based on SVD feature extraction and transfer learning classification," in *Proceedings of the 2015 Prognostics and System Health Management Conference (PHM)*, pp. 1–6, IEEE, Beijing, October 2015.

[12] D. T. Hoang and H. J. Kang, "A Motor current signal based bearing fault diagnosis using deep learning and information

fusion," *IEEE Transactions on Instrumentation and Measurement*, vol. 69, no. 6, pp. 3325–3333, 2020.

[13] V. C. M. N. Leite, J. G. B. da Silva, G. L. Torres et al., *Bearing Fault Detection in Induction Machine Using Squared Envelope Analysis of Stator Current,"* Bearing Technology*, Springer, Berlin, Germany, 2017.

[14] E. Elbouchikhi, V. Choqueuse, F. Auger, and M. E. H. Benbouzid, "Motor current signal analysis based on a matched subspace detector," *IEEE Transactions on Instrumentation and Measurement*, vol. 66, no. 12, pp. 3260–3270, 2017.

[15] B. R. Nayana and P. Geethanjali, "Analysis of statistical time-domain features effectiveness in identification of bearing faults from vibration signal," *IEEE Sensors Journal*, vol. 17, no. 17, pp. 5618–5625, 2017.

[16] G. Maruthi and V. Hegde, "Application of mems accelerometer for detection and diagnosis of multiple faults in the roller element bearings of three phase induction motor," *IEEE Sensors Journal*, vol. 16, no. 1, pp. 145–152, 2016.

[17] J. Tian, C. Morillo, M. H. Azarian, and M. Pecht, "Motor bearing fault detection using spectral kurtosis-based feature extraction coupled with k-nearest neighbor distance analysis," *IEEE Transactions on Industrial Electronics*, vol. 63, no. 3, pp. 1793–1803, 2016.

[18] C. P. Mbo'o and K. Hameyer, "Fault diagnosis of bearing damage by means of the linear discriminant analysis of stator current features from the frequency selection," *IEEE Transactions on Industry Applications*, vol. 52, no. 5, pp. 3861–3868, 2016.

[19] D. Pasqualotto and M. Zigliotto, "Increasing feasibility of neural network-based early fault detection in induction motor drives," *IEEE Journal of Emerging and Selected Topics in Power Electronics*, vol. 10, no. 2, pp. 2042–2051, 2022.

[20] J. Pons-Llinares, J. A. Antonino-Daviu, M. Riera-Guasp, S. Bin Lee, T.-J. Kang, and C. Yang, "Advanced induction motor rotor fault diagnosis via continuous and discrete time–frequency tools," *IEEE Transactions on Industrial Electronics*, vol. 62, no. 3, pp. 1791–1802, 2015.

[21] K. N. Gyftakis, J. A. Antonino-Daviu, R. Garcia-Hernandez, M. D. McCulloch, D. A. Howey, and A. J. M. Cardoso, "Comparative experimental investigation of broken bar fault detectability in induction motors," *IEEE Transactions on Industry Applications*, vol. 52, no. 2, pp. 1452–1459, 2016.

[22] D. Pasqualotto and M. Zigliotto, "A comprehensive approach to convolutional neural networks-based condition monitoring of permanent magnet synchronous motor drives," *IET Electric Power Applications*, vol. 15, no. 7, pp. 1–16, 2021.

[23] S. Selvarajan, H. Manoharan, T. Hasanin et al., "Biomedical signals for healthcare using hadoop infrastructure with artificial intelligence and fuzzy logic interpretation," *Applied Sciences*, vol. 12, no. 10, p. 5097, 2022.

[24] H. Manoharan, S. Selvarajan, A. Yafoz et al., "Deep conviction systems for biomedical applications using intuiting procedures with cross point approach," *Frontiers in Public Health*, vol. 10, p. 909628, 2022.

[25] G. B. Mohammad, S. Shitharth, S. A. Syed et al., "Mechanism of internet of things (IoT) integrated with radio frequency identification (RFID) technology for healthcare system," *Mathematical Problems in Engineering*, vol. 2022, pp. 1–8, Article ID 4167700, 2022.

[26] B. D. E. Cherif, M. Chouai, S. Seninete, and A. Bendiabdellah, "Machine-learning-based diagnosis of an inverter-fed induction motor," *IEEE Latin America Transactions*, vol. 20, no. 6, pp. 901–911, 2022.

[27] R. R. Kumar, V. Randazzo, G. Cirrincione et al., "Induction machine stator fault tracking using the growing curvilinear component analysis," *IEEE Access*, vol. 9, pp. 2201–2212, 2021.

[28] B. Gou, Y. Xu, Y. Xia, Q. Deng, and X. Ge, "An online data-driven method for simultaneous diagnosis of igbt and current sensor fault of three-phase pwm inverter in induction motor drives," *IEEE Transactions on Power Electronics*, vol. 35, no. 12, pp. 13281–13294, 2020.